X-ray-absorption near-edge structure of titanium and vanadium in $(Ti,V)O_2$ rutile solid solutions

B. Poumellec, J. F. Marucco, and B. Touzelin
Laboratoire des Composés Non-Stoechiométriques, Université de Paris—Sud, Bâtiment 415, 91405 Orsay Cédex, France
(Received 22 January 1986; revised manuscript received 19 September 1986)

An improved smoothing procedure is used to extract more information from x-ray-absorption spectra by second-derivative analysis. The true energy position of the maxima and full width at half maximum are measured for all features. The excitonic peak is present for all compositions and is well correlated with the $3d$-electron density. A weak structural change appears around the titanium atom whereas a structure change is more detectable around the vanadium atom. The crystal-field splitting seems to be largely determined by V-V interactions. No electron transfer occurs between titanium and vanadium as the V $3d$ level is about 1 eV below the Ti $3d$ level. This is done by aligning the two edges with a 498.3-eV shift.

I. INTRODUCTION

TiO_2 has been largely studied in the past as an oxygen sensor and for other applications. VO_2 shows a semiconductor-metal transition at 341 K and much research has been done on this fundamental problem. On the other hand, $(Ti,V)O_2$ solid solutions have been less thoroughly investigated. Generally, all solid solutions are less studied because of their structural disorder. In $(Ti,V)O_2$, titanium and vanadium atoms belong to the same sublattice with probably a random distribution on the sites.[1]

X-ray-absorption spectroscopy, which is a local probe, is a useful tool for studying titanium and vanadium separately, along with their nearby surrounding atoms. Moreover, x-ray diffraction averages the crystal disorder and shows only the long-range order.

TiO_2 crystallizes at high temperature in rutile form [space group D_{4h}^{14} ($P4_2/mnm$)]. The coordination oxygen octahedron is slightly distorted, i.e., four Ti-O distances are 0.193 nm and two others are 0.201 nm.[2] VO_2 crystallizes above 341 K in rutile form with four 0.190-nm and two 0.195-nm V-O distances.[3] Below 341 K, VO_2 is monoclinic, which is a distorted rutile structure [space group C_{2h}^5 ($Pmma$)] due to a small shift of vanadium atoms along the c axis.[3] There are two vanadium sites, which are symmetric by point inversion.[4] The four equal V—O bonds in rutile become 0.187, 0.1865, 0.201, and 0.204 nm, and the two others 0.205 and 0.1763 nm. This significant distortion splits the V-V distances in rutile form (0.288 nm) into two alternate distances (0.265 and 0.312 nm). The shortening of V—V bonds and the electron-electron correlations give rise to a gap[5] of the order of 0.5 eV which opens in the d band, and leads to semiconducting properties.

In $(Ti,V)O_2$, x-ray-diffraction data indicate that solid solutions have rutile form below $x=0.80$ and are monoclinic above it.[6] The aim of this paper is to detect changes in x-ray-absorption near-edge structure related to the above-mentioned distortion of the oxygen octahedron, and possibly to changes in the electronic density of states.

II. EXPERIMENT

X-ray-absorption edge spectra were recorded at Laboratoire pour l'Utilisation due Rayonnement Electromagnétique (LURE) Orsay, with DCI-storage-ring synchrotron radiation on the EXAFS2 beam line with a 0.2-eV energy step. The two crystals of the monochromator were Si(3,1,1), referenced to the $A2$ peak at 4967.75 eV of TiO_2; the slit entrance was 0.5 mm. The harmonics above 6 keV were suppressed by two parallel glass mirrors, an improvement made by Goulon and Cortes.

A. Sample preparation and experimental spectra

Stoichiometric samples were obtained from the oxydoreduction process described in Refs. 6 and 7. After milling, the powders were dusted onto several pieces of Scotch tape until a reasonable absorption step was obtained. This procedure has the disadvantage of creating a nonuniform specimen due to variations in the powder-layer thickness. To avoid relative intensity errors between preedge and edge, several spectra were recorded at various positions to test the reproducibility.

Spectra were recorded from 4950 to 5020 eV for the Ti edge and from 5440 to 5520 eV for the V edge. The absorption was normalized by subtracting from $\mu(E)=\ln(I_0/I)$ the background $\mu_0(E)$ estimated from the linear mean-square fit at 20 eV before the edge and then by dividing $\mu(E)-\mu_0(E)$ by its maximum value. A better procedure would be to estimate the jump by recording the spectra far above the edge as in Ref. 8, but in the present case it was not useful since the variations are rather small over all the spectra.

B. An improved smoothing procedure

After this shaping process, we used an improved smoothing procedure to obtain second derivatives. We think the second derivative is easier to interpret and requires no constraining hypotheses.

The classical way of finding the derivatives is to compute $[\mu(E+\Delta)-\mu(E)]/\Delta$, where Δ is the energy step,[8] but this yields a non-noisy first derivative only if the absorption spectrum is perfect. In any case, using the same procedure on the first derivative gives rise to a noisy second derivative. For dilute atoms, spectra are often noisy.

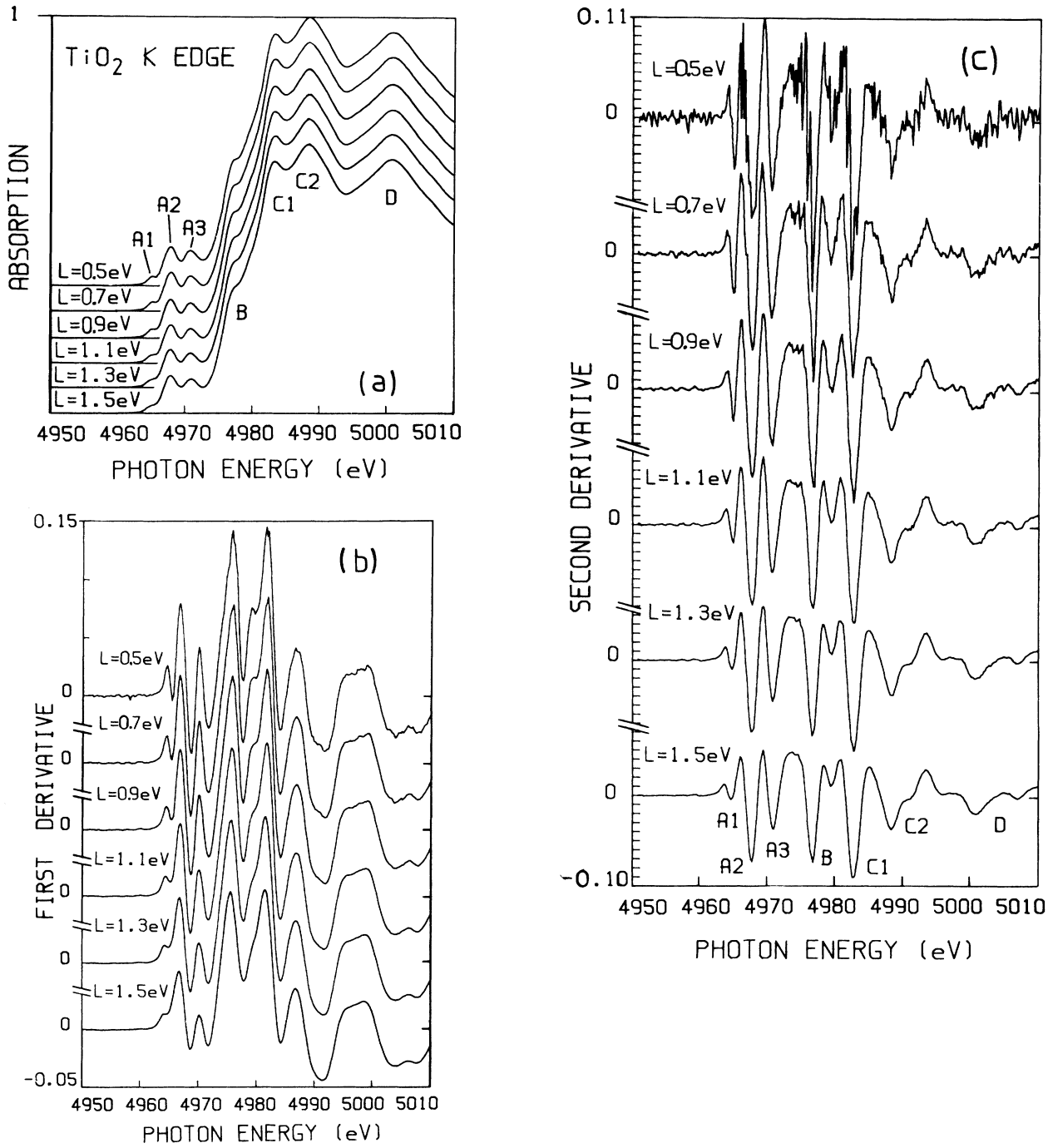

FIG. 1. (a) X-ray absorption at Ti K edge in TiO_2 versus the width of the smoothing window from $L=0.5$ to 1.5 eV. (b) First derivative of the absorption with respect to the smoothing window. (c) Second derivative of the absorption with respect to the smoothing window.

A first improvement of the above-mentioned method is to find a linear least-mean-squares fit on consecutive points having the energy between $E-L$ and $E+L$, where L can be a multiple of the energy step. L is chosen to be minimum, in order to not decrease the resolution. Nevertheless, this improvement does not give the second derivative directly. A further improvement can be made by applying a second-degree mean-squares fit to the points lying between E_0-L and E_0+L, with E_0 being between the minimum and the maximum photon energy.

Locally we have

$$\mu(E)=A(E-E_0)^2+B(E-E_0)+C \ ;$$

then

$$\mu(E_0)=C, \quad \frac{d\mu(E_0)}{dE}=B, \quad \frac{d^2\mu(E_0)}{dE^2}=2A \ .$$

L is taken at the minimum value to obtain a satisfactory second derivative. It is worth noting that E_0 is the middle of the energy interval and is fixed *a priori*. The only input data required are the values of A, B, and C. This type of sampling is better than taking a fixed number of points, because the actual energy step is not regular.

Moreover, as the smallest possible L value should be used, several spectra of the same sample must be recorded if the noise is too large (this is the case for the dilute sample, such as, for instance, the V K edge with $x=0.1$). But since the energy step is irregular, the added intensity from point to point introduces errors. It is thus better to gather the different spectra available and sort the data by increasing energy, to obtain a new spectrum. There are now several times more points between $E-L$ and $E+L$ and the smoothing procedure is then applied. Statistically, this procedure is quite satisfactory. Details concerning this point are given in Ref. 9, which also deals with x-ray-absorption near-edge spectroscopy (XANES) in $(Ti,Ta)O_2$ solid solutions.

C. Critical application of the smoothing procedure

We want to show the various effects of the smoothing, to reach firm conclusions.

We analyze the well-known Ti K edge of rutile TiO_2.[10] In Fig. 1 the absorption and the first and second derivatives are shown versus the half-width of the window L.

For $L=0.5$ eV the coefficients A, B, and C are determined from ten experimental points. The absorption spectrum for that width of the window is reconstructed quite well. The first derivative is not very noisy but the second one is not well defined. An improvement is obtained by widening the window to 0.7 eV. Moreover, for the Ti K edge it is not useful to increase the width of the window further. Using the wider window, the spectra are better concerning noise, but not for relative intensity.

In the absorption curve the intensity of the first weak peak ($A1$) decreases as L increases. In the first derivative curve, $A1$ disappears progressively and $A2$ and $A3$ are also altered but not shifted. In the second derivative, for windows wider than, 0.7 eV, all XANES features appear clearly. Although the intensity of the overall second derivative decreases, only small changes are detectable in the relative intensity of the different features.

On the other hand, for a given energy the value of the second derivative represents the local concavity of the absorption spectrum. The maximum of the absorption spectrum does not indicate the real energy position of the peak because it is often perturbed by a neighboring structure (B, for instance); however, the negative minimum of the second derivative does. It is worth noticing, for instance, that B is well defined on the second derivative, whereas it is only a shoulder on the absorption spectrum. The energy positions of the negative minima are not altered by the increase of the width of the window, except for the $A1$ peak, which is shifted towards lower energies for $L>1.3$ eV. Lastly, if we assume a Lorentzian form of the absorption peak, the full width at half maximum (FWHM) can be estimated by the zeros on each side of a negative minimum of the second derivative which correspond to full width between inflection points (FWIP). It can be shown that

$$W(\text{FWHM})=1.7W(\text{FWIP}) \ .$$

Table I shows that a FWHM increase of a few tenths of an eV is possible with increasing L, but surprisingly it is not found for the narrowest peaks. A FWHM measurement is no longer significant as L increases above the FWHM for a given peak. For instance, to reconstruct the $A1$ peak, L must be smaller than 1.3 eV. (Note the window in which the second-degree polynomial is computed is $2L$ and thus may be wider than he FWHM but no more than twice as wide.)

Figure 2 shows the V edge of VO_2. The $A1$ structure is easy to detect on the second derivative, although it was

TABLE I. Apparent full width at half maximum (eV) versus the width of the smoothing window L, in eV, for the main XANES features.

	Peak label					
L	$A1$	$A2$	$A3$	B	$C1$	$C2$
0.7	1.3	3.2	2.6	2.9	4.0	
0.9	1.3	3.2	2.6	2.9	4.0	7.8
1.1	1.3	3.2	2.6	3.2	4.0	
1.3	1.3	3.2	2.6	3.4	4.2	
1.5	1.1	3.2	2.6	3.4	4.2	

TABLE II. Full width at half maximum (eV) versus the composition for the Ti edge in $Ti_{1-x}V_xO_2$.

	Peak label					
x	$A1$	$A2$	$A3$	B	$C1$	$C2$
0	1.3	3.2	2.6	2.9	4.0	7.8
0.1	1.3	3.4	2.8	2.9	4.1	8.0
0.55	1.1	3.6	2.8	2.9	4.1	8.3
0.87	1.1	3.4	2.6	2.9	4.1	8.5

not mentioned previously.[11] This confirms the usefulness of our procedure.

III. SPECTRUM ANALYSIS

Three solid solutions $Ti_{1-x}V_xO_2$ are analyzed ($x=0.1, 0.55, 0.87$) in addition to TiO_2 and VO_2. All of the spectra show the weak peaks $A1$, $A2$, and $A3$ before the edge, the B shoulder on the edge, the strong peaks $C1$ and $C2$ at the edge, and the D peak away from the edge. In fact, $C2$ splits into the $C2'$ and $C2''$ peaks, and D also.

With a Si(3,1,1) monochromator the $A1$ peak of the Ti K edge in TiO_2 is better resolved than with Si(1,1,1) (Fig. 1).[10] This is due to the better resolution. The other features are quite similar to those previously published.

The VO_2 spectrum (Fig. 2) also agrees with the one shown by Bianconi *et al.*,[11] except that we can detect the $A1$ peak on the second derivative, whereas it was not visible previously. In fact, it is not visible on either the absorption spectrum or the first derivative. Only the second derivative reveals its presence.

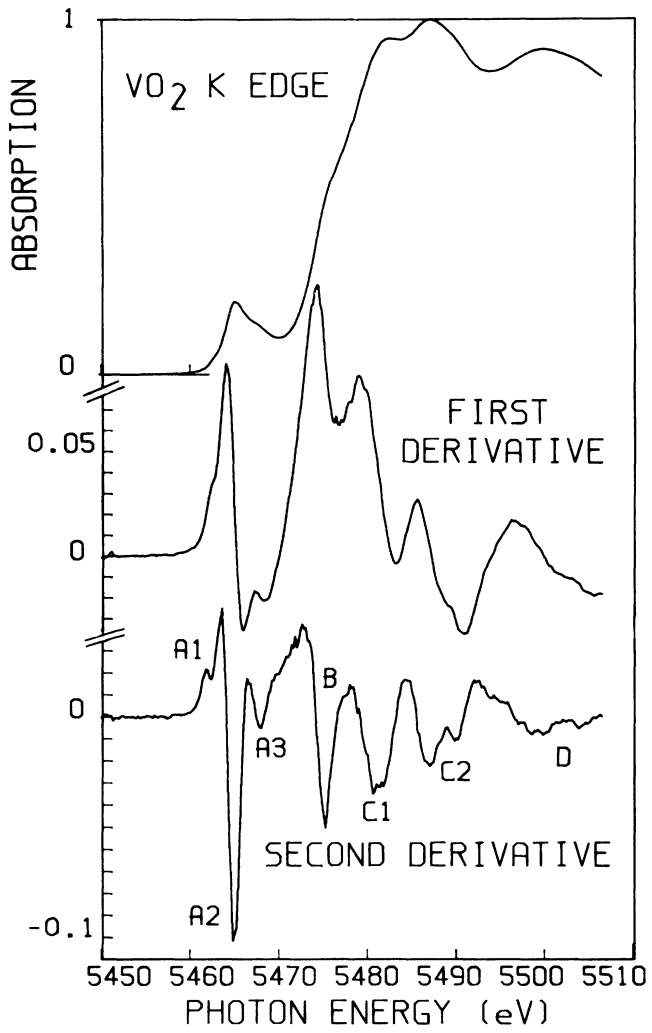

FIG. 2. X-ray absorption and derivatives at V K edge in VO_2. $L=0.7$ eV for the absorption and the first derivative; $L=1.1$ eV for the second derivative.

A. Analysis of the Ti edge (Fig. 3)

The width of the window is $L=0.9$ eV (see Fig. 3). The $A1$ peak progressively disappears with increasing vanadium content. The $A2$ and $A3$ peaks also decrease in intensity. The other features are not modified. Table II shows that the FWHM does not change much with vanadium content except for the $C2$ peak. $A1$ is always the narrowest peak, and $A2$, $A3$, and B are rather narrow compared to $C1$ and $C2$.

In Fig. 3(c) we plot the energy positions of the different XANES features. Only $A1$ and $A2$ are weakly shifted to lower energy when the vanadium content increases. The splitting between $A2$ and $A3$ seems to increase by 0.2 eV but this is of the order of magnitude of our resolution.

B. Analysis of the V edge (Fig. 4)

The width of the window was $L=1.1$ eV for $x=1$, 0.87, and 0.55, and $L=1.5$ eV for $x=0.1$ (see Fig. 4). The window is wider than for the Ti edge because the atomic absorption is lower.

On the absorption spectra, the $A1$ peak is not visible but all others are present. The intensity of $A2$ increases with vanadium content. On the second derivative, the $A1$ peak appears progressively with vanadium content but remains a small feature contrary to the Ti edge. The D peaks do not split clearly any more. The intensity of $A3$ is weak and shifts to lower energy.

Table III shows that all the peaks are broader than for the Ti edge, but B remains narrower than $A2$. Figure 4(c) shows the energy position of the different XANES features. As found for the Ti edge, B, $C1$, and $C2$ do not shift with vanadium content. On the other hand, the splitting of $A2$ and $A3$ decreases as the vanadium content increases, contrary to what is observed at the Ti edge.

C. Chemical shift

When the valence of the atom changes, the edge shifts by an amount of 1 eV per ionization degree at 5 keV.[8,11] The positive shift of the edge with the valence increase is related to an increase in the attractive potential of the nucleus on the $1s$ core electron and to a reduction in the repulsion core Coulomb interaction with all other electrons in the compound. This valence effect shifts the whole spectrum. The problem is then to distinguish this shift from shifts due to other effects. Since only three features shift, we conclude that no valence change occurs and $3d$ electrons are principally localized on vanadium. This result is in agreement with conclusions drawn from magnetic-susceptibility experiments.[1]

IV. DISCUSSION

A. One-electron transitions

In the one-electron (or single-particle) transition model, it is assumed that only one core electron is excited to an unfilled state of the unperturbed solid. The remaining electrons are assumed to be unaffected, and frozen in their original state. Many-body corrections, including relaxation of the valence electrons in response to the core-hole

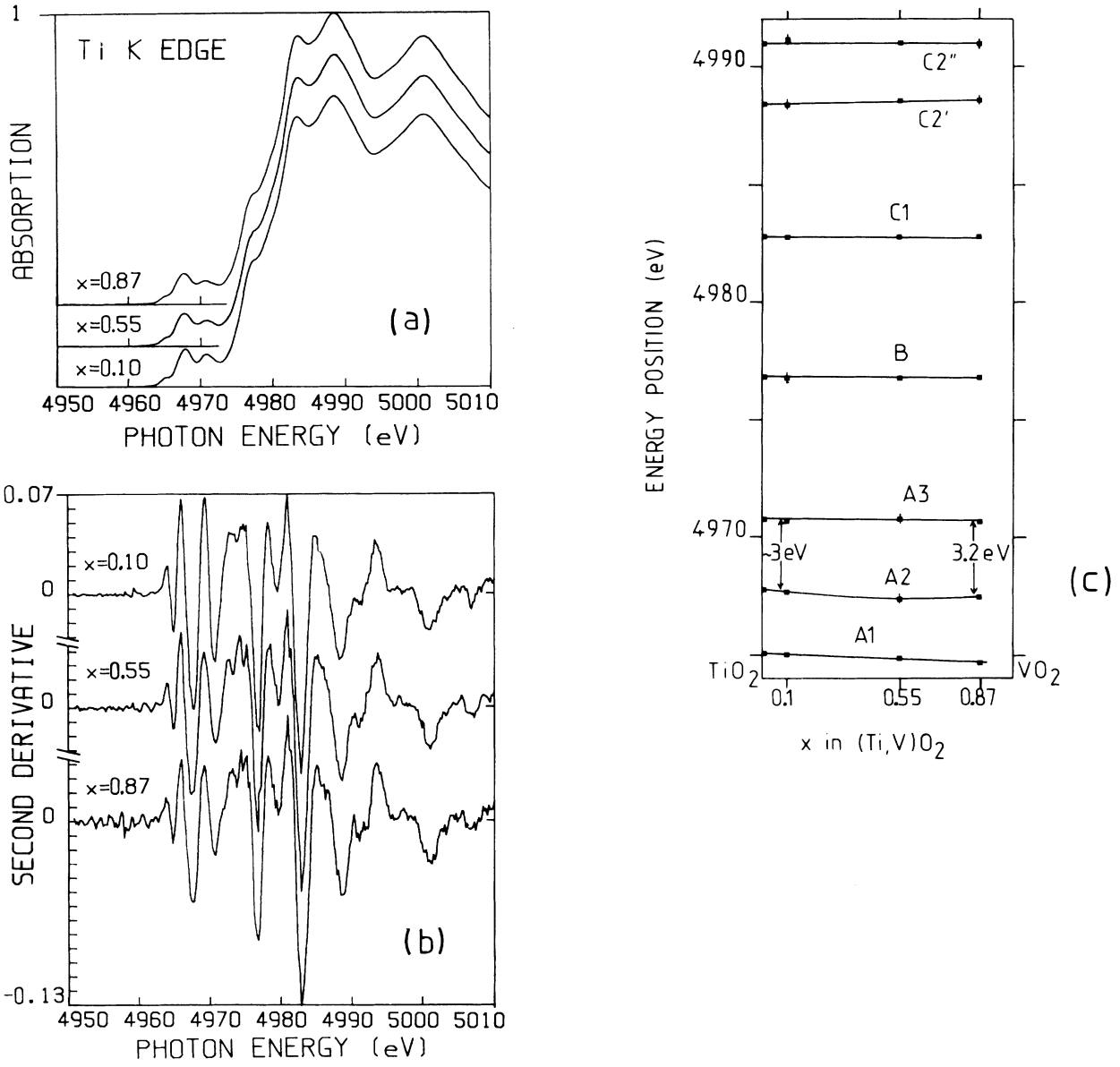

FIG. 3. (a) X-ray absorption at Ti K edge in $Ti_{1-x}V_xO_2$. (b) Second derivative with respect to the composition. (c) Peak position at Ti K edge with respect to the composition for $Ti_{1-x}V_xO_2$.

and excited-electron—core-hole interactions, alter the one-electron picture, but these corrections will be ignored for the moment. Because the initial-state core levels are tightly bound, they have narrow energy widths and are therefore essentially structureless. Hence the core edges are expected to reflect the unfilled conduction-band density of states (DOS) in the solid, or rather its symmetry-projected components (PDOS) due to the dipole or quadrupole selection rules. The metal K edges arise primarily from $1s \rightarrow 4p$ dipolar transitions, although it appears that the features observed at threshold may be due to $1s \rightarrow 3d$ quadrupolar transitions. A first approach for explaining the XANES features can be made by reference to the local symmetry around the metal atoms near the edge. In rutile structures, the point group is D_{2h} (mmm) and the coordination octahedron around the titanium is distorted. We have the symmetry-scheme correlation between R_3, O_h ($m3m$), and D_{2h} shown in Fig. 5. Band-structure calculations indicate that the t_{2g} and e_g manifolds do not mix; their splitting is of the order of 3 eV.[12,13] The symmetry lowering ($O_h \rightarrow D_{2h}$) is not enough to give rise to detectable splittings of t_{2g} and e_g levels in our experiment[14] (the

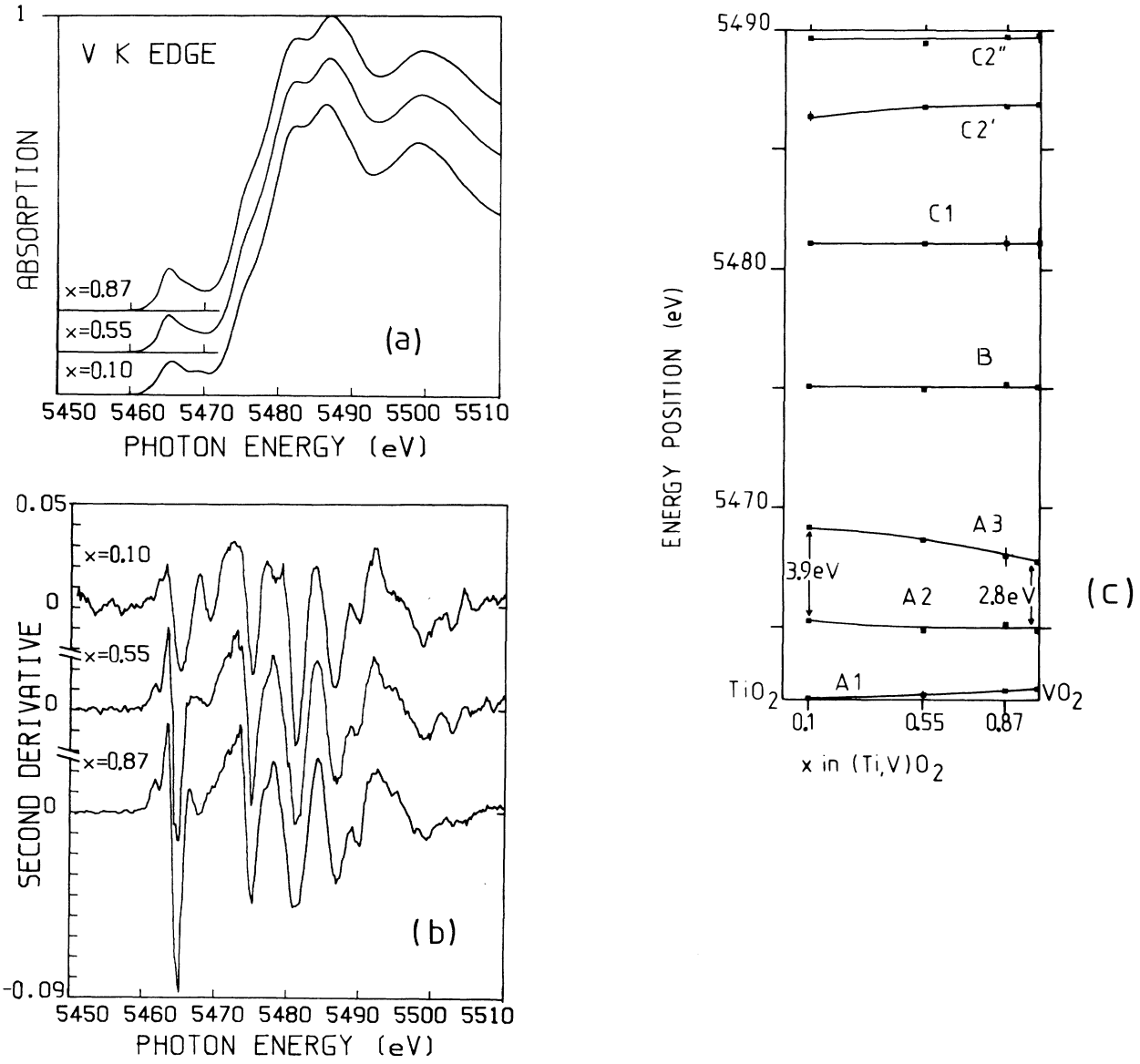

FIG. 4. (a) X-ray absorption at V K edge in $Ti_{1-x}V_xO_2$. (b) Second derivative with respect to the composition. (c) Peak positions at V K edge with respect to the composition for $Ti_{1-x}V_xO_2$. The A positions are estimated as there is no negative minima on the second derivative.

TABLE III. Full width at half maximum (eV) versus the composition for the V edge in $Ti_{1-x}V_xO_2$.

	Peak label					
x	$A1$	$A2$	$A3$	B	$C1$	$C2$
0.1		4.9		3.1	6.5	8.8
0.55		3.1		3.1	6.5	8.8
0.87		3.6		3.6	4.9	9.3
1.0		3.4		4.3	7.0	9.0

splitting is smaller than the experimental resolution by about 0.2 eV). Hence the following assignment can be proposed:

$A2$: $1s \rightarrow t_{2g}$,

$A3$: $1s \rightarrow e_g$.

As the energy of the photoelectron increases, its mean free path decreases from about 100 to 10 Å. Therefore, a cluster calculation including several shells of neighbors is probably good enough to compute the absorption. Kutzler *et al.*[15] have performed discrete-variation-method (DVM) one-electron calculations (ignoring the core-hole potential) for TiO and VO (cubic cell) using a 27-atom cluster centered on the transition-metal atom. They obtain two maxima very similar to our $C2$ and D peaks by using $4s$ and $4p$ virtual orbitals. On the other hand, Bair *et al.*[16] have computed the dipole and quadrupole K-shell transitions of Cu^{2+} by the self-consistent-field (SCF) method. We assume that the energy position of transitions above $1s \rightarrow 4p$ does not change much within the first row of transition metals. According to the work of Bair *et al.*,[16] the $1s \rightarrow 4p$ transitions should appear at about 17 eV above the $1s \rightarrow e_g$ transitions. This corresponds to a $C2'$ peak, which is the strongest. The transition $1s \rightarrow 5p$ is found to be at about 28 eV and the $1s \rightarrow 6p$ at about 32 eV above the $1s \rightarrow 3d$ transitions,[16] and thus these transitions would fall in the region of the D peaks and above it.

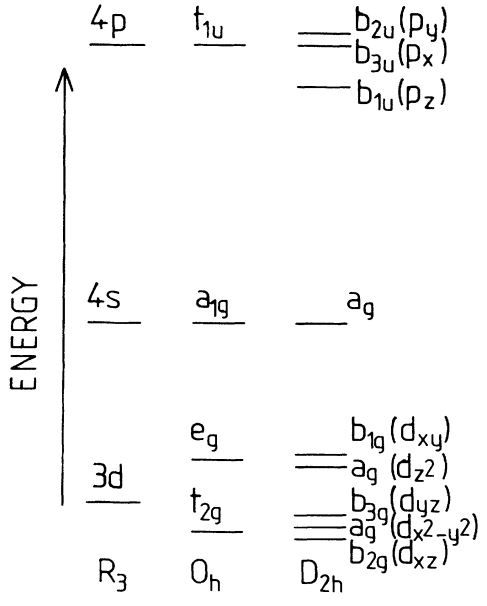

FIG. 5. Schematic diagram of symmetry correlations when the symmetry is lowered from free-ion, octahedral, and orthorhombic symmetry.

B. Multielectron effects

1. *Excitons*

In insulators, band gaps of a few eV open up between the filled valence and unfilled conduction bands. Hence the excited electron is poorly screened from the core hole by the valence electrons, and the one-electron transition model is no longer satisfactory. In some cases, the hole may have a potential strong enough to bind the excited electron. Such a two-particle state is known as a (Frenkel) core exciton and often has an excitation energy below the one-electron threshold (Frenkel core excitons are highly localized in contrast to the lower-energy Wannier valence excitons, for which the excited electron is not localized in the vicinity of the core hole.) Upon formation of such core excitons, the dipole selection rule still holds. However, the symmetry-projected final states of the transitions are not those of the unperturbed initial solid. They are determined by the solid containing a partially screened, relaxed core hole. The energy difference between the levels obtained by switching the core-hole potential on or off is expected to decrease when the overlapping between neighbor orbitals increases, i.e., it will be greater for $3d$ than for $4p$ bands. The $3d$ orbitals of the excited atom are more sensitive to the core-hole potential than the $3d$

TABLE IV. Estimated binding energy (E_b), in eV, of the $A1$ exciton versus the composition at the Ti and V edges.

	x				
	0.0	0.1	0.55	0.87	1.0
E_b at Ti edge	1.2	1.0	0.8	1.1	
E_b at V edge		0.85	0.95	0.80	0.80

orbitals of the neighbors. If the screening is weak, the attractive core-hole potential gives rise to a level below the conduction bands. The PDOS of the solid is therefore made up from discrete levels (bound exciton) and from bands. If the overlapping between metallic neighbors is very weak, the PDOS of band states is zero. Conversely, if the overlapping is large, there is no discrete level. Intermediate situations may give rise to the presence of both structures.

We think that the $A1$ peak appearing on almost all spectra could be the lowest excitonic level. The FHWM of this structure is about 1.3 eV and compares well with the combination of the lifetime broadening of the core hole (~ 1 eV) and the experimental resolution (~ 0.7 eV). According to the excited atom, the $A2$ (or $A3$) peaks can be assigned to the titanium or vanadium part of the t_{2g} (or e_g) band transitions. We propose that the $A1$ peak corresponds to the $1s \rightarrow t_{2g}$ excitonic transition, while the $1s \rightarrow e_g$ excitonic transition could be merging in the $1s \rightarrow t_{2g}$ band transitions.

The exciton binding energy is the difference between the energy of the first-exciton line and the bottom of the titanium or vanadium part of the conduction band. It amounts to a few tenths of an eV. Screening of the core potential by valence electrons decreases the binding energy of the exciton. For a semiconductor with a wide band gap such as TiO_2 (3 eV),[17] the screening is small and the exciton $A1$ appears clearly. The binding energy E_b can be estimated from the FWHM of $A2$, and the energy position of $A1$ by the following expression,

$$E_0 = [E_{A2} - E(\mathrm{FWHM}(A2))/2] - E_{A1} ,$$

assuming that the bottom of the conduction band is almost at the energy corresponding to the half-height of $A2$. Results are shown in Table IV.

The binding energy of the exciton seems to decrease at the Ti edge, at least from TiO_2 solid solutions with V content up to $x = 0.55$, whereas it increases at the V edge. This is well correlated with the intensity change of the $A1$ peak. The variations in the binding energy are related to the variation in the screening by valence electrons. It is worth noting that no electron is present in the $3d$ orbital in TiO_2, whereas V^{4+} is a $3d^1$ ion. Thus, the number of electrons in the vicinity of the conduction band (and so the screening increases with the vanadium content. Even if the vanadium $3d^1$ electron is spatially localized, the conductivity increases with vanadium content up to $x = 0.72$,[18,19] and thus electrons are present a small part of the time on titanium. Therefore, the screening effect is stronger on vanadium than on titanium and the binding energy is smaller at the V edge than at the Ti edge. Incidentally, it is surprising that the exciton can even be detected, since it could be screened by the $3d$ valence electron. The reason why the exciton is still detected is that d electrons are essentially localized at room temperature, as in low-temperature VO_2.[17] The localization arises from the antiferromagnetic coupling between vanadium neighbors. Interaction between the core hole and the $3d$ electron is therefore too weak to produce a strong screening effect. It is the opposite situation in metallic VO_2,[11] or in VO, TiO, or Ti,[20] for which the $A1$ peak is undetectable.

2. *Other multielectron transitions*

In the above analysis, two peaks remain unassigned: B and $C1$. The B peak is the hump on the edge. Fisher[21] and Grunes[10] mentioned that it could be ascribed to the $1s \rightarrow 4s$ transitions and, actually, it falls at the correct calculated energy. But, the $1s \rightarrow 4s$ transition is completely forbidden except in D_{2h} symmetry (see Table V); hence a strong vibronic coupling (mixing about 10% of b_{1u} symmetry) (Ref. 16) is required to give rise to the observed intensity of the B peak. Since this hump is a quasiuniversal feature on K edges, sometimes accompanied by other satellites, it remains unexplained.

In a preceding section we discussed spectra according to the one-electron approximation, and this is a useful tool in predicting the intensity of a large portion of the XANES. Nevertheless, multielectron processes should be considered. The exciton is one example, a multiplet splitting of final-state configurations is another. Bianconi[11] explains the vanadium preedge structures of metallic VO_2 by such a phenomenon. The splitting in the excited state can arise from the difference of localization and overlapping of the d subbands. The more localized a subband is, the more it is lowered by the attractive core-hole potential. This leads to a splitting of the t_{2g} band in the excited state. This does not seem to occur in the low-temperature form of VO_2 and of solid solutions. Bair *et al.* have found by self-consistent-field (SCF) calculations with configuration interactions that the $1s^1$-$3d^{10}\underline{L}^1$ metallic configuration is more stable than $1s^1$-$3d^9$ in $CuCl_2^+$, the d electron coming from the highest occupied orbitals (L) of

TABLE V. Selection rules for transitions in D_{2h} symmetry. a means allowed, f means forbidden.

	a_g:		t_{2g}		e_g		a_{1g}		t_{1u}	
	$1s \rightarrow$	$1b_{2g}$	$1a_g$	$1b_{3g}$	$2a_g$	$1b_{1g}$	$3a_g$	$1b_{1u}$	$1b_{3u}$	$1b_{2u}$
Dipole	$b_{1u}(z)$	f	f	f	f	f	f	a	f	f
	$b_{2u}(y)$	f	f	f	f	f	f	f	f	a
	$b_{3u}(x)$	f	f	f	f	f	f	f	a	f
Quadrupole	$b_{1g}(xy)$	f	f	f	f	a	f	f	f	f
	$b_{2g}(xz)$	a	f	f	f	f	f	f	f	f
	b_{3g}	f	f	a	f	f	f	f	f	f
	$a_g(x^2,y^2,z^2)$	f	a	f	a	f	a	f	f	f

the ligand ($\underline{L}$ denotes a hole in the valence band). This two-electron excitation is called a shakedown. On the other hand, Kosugi,[22] by comparing theoretical calculations with experimental polarized spectra of Cu II flat complexes, reached the conclusion that each $1s \rightarrow np$ transition splits in two: the normal transition and another one with a simultaneous excitation of one ligand electron to the $3d$ band. From Kosugi, a shakedown transition is found at about 6—9 eV below the normal transition; hence $C2''$ could be the $1s \rightarrow 5p$ shakedown 9 eV below $1s \rightarrow 5p$, and $C1$ could be the $1s \rightarrow 4p$ shakedown 6 eV below $1s \rightarrow 4p$. Shakedown transitions are also mentioned by Grunes[10] for many insulating compounds to explain part of the C or D group or the B hump. Without ignoring the possibility of charge transfer in the excited state, we must note that $3d^{10}$ is a closed shell and could stabilize the excited configuration versus the $3d^9$ one. Such stabilization is not possible in our compounds, where the transition metals have $3d^0$ or $3d^1$ configurations in the fundamental state. Clearly, more theoretical calculations are required to interpret the observed $(1s \rightarrow p)$-type transitions.

C. Structural information

Natoli[23] has shown that the energy difference between excitonic or bound and continuum resonance is inversely proportional to the squared mean O-M distances. Previous discussion on binding energy implies that care must be taken in the choice of the features used in computing the mean distance. The result will be different if we choose the exciton line, which shifts relative to $C1$ but not to $C2$, or the $1s \rightarrow t_{2g}$ transition. We think that $A2$ is a good bound resonance approaching the Fermi level, but not the exciton line, because of the effect of screening described in Sec. IV B. Then which continuum resonance should we choose?

Table VI shows that all energy shifts correspond to a squeezing of the coordination octahedron, but their magnitude is quite different depending on how the transitions are paired. Table VII shows that the mean M—O bond length decreases from TiO_2 to VO_2 by 0.0024 to 0.0040 nm. It is worth noting that M-$O_{||}$ decreases by 0.0010 nm, whereas M-$O_{\perp}$ remains almost constant. Moreover, the octahedron in TiO_2 is stretched in the direction of the z axis, whereas it is flattened in monoclinic VO_2; therefore

TABLE VI. Variation of the mean M—O bond length (in mn) as suggested by Natoli (Ref. 22) and deduced from the energy position of C peaks with respect to $A2$ from TiO_2 to VO_2. The difference between the energy positions of peaks is inversely proportional to the squared radius. The coefficient of proportionality is calculated in TiO_2 or VO_2 knowing the M—O bond length. (CP denotes coefficient or proportionality.)

	Ti edge	V edge	Error
CP (eV mm^2)	0.792	0.810	
$C2''$% $A2$	−0.0013	−0.0016	0.0004
$C2'$% $A2$	−0.0024	−0.0037	0.0005
$C1$% $A2$	−0.0019	−0.0019	0.0006

TABLE VII. Mean atomic distances in TiO_2 and rutile and monoclinic VO_2.

	M-$O_{||}$	M-$O_{\perp}$	M-O	M-M
TiO_2	0.201	0.193	0.1957	0.2958
Rutile VO_2	0.195	0.190	0.1917	0.2869
Monoclinic VO_2	0.1907	0.1946	0.1933	0.289
				(0.256—0.312)

b_{1u} in Fig. 5 rises above b_{2u} and b_{3u}. If Natoli's relation is valid, we then expect a shift of all $1s \rightarrow np$ peaks relative to $1s \rightarrow t_{2g}$ due to the same variation of mean bond length. Clearly, this is not the case, because the two effects are operative.

The absorption peaks probably do not all have the same polarization. The calculation of the energy position of the polarized transitions by Kosugi[22] for flat Cu II complexes, which is representative of an infinite distortion of the octahedron by stretching, shows that the $1s \rightarrow 5p$ transition is quasi-independent of the polarization and hence of the mean radius, whereas this is not so for $1s \rightarrow 4p$. Thus Natoli's suggestion breaks down for the former transition, but it should be valid for the $1s \rightarrow 4p$ direct transition. Therefore, we conclude that the V octahedra are more enlarged than the Ti octahedra. This conclusion agrees with the fact that M-O in TiO_2 is shorter than in VO_2.

Furthermore, for $(Ti,Nb)O_2$ we find an increase of 0.011 nm around the titanium as the Nb content increases. (The mean M-O distance in NbO_2 is 0.206 nm).[24]

D. Electronic-structure information

The splitting of t_{2g} and e_g is the crystal-field splitting, i.e., $A2$ and $A3$ splitting [Fig. 3(c)]. It has almost a constant value of about 3.1 eV around titanium, whereas it decreases from 3.9 to 2.8 eV around vanadium. For $x < 0.8$ the local symmetry around the metallic atoms is D_{2h}. The calculations of Burton and Cox[13] show that the orthorhombic splitting of t_{2g} in VO_2 is smaller than 0.075 eV. This is well below our resolution. This result is confirmed by the cluster calculation of Lazukova *et al.*,[25] who find 4 eV between t_{2g} and e_g for rutile VO_2, in agreement with the observed value.

For $x > 0.8$ all symmetry breaks down; but this gives rise only to a splitting smaller than 0.17 eV. Hence the splitting between $A2$ and $A3$ seems to correspond mainly to the octahedral crystal-field splitting. It is 2.8 eV in VO_2, and this value agrees well with the cluster calculation of Burton and Cox, who found 2.7—3.0 eV.[13]

Then how can we explain the discrepancy between titanium and vanadium? The distortion of the coordination octahedron is rather small and such that the crystal-field splitting should increase when the mean size of the octahedron decreases. This applies to $(Ti,Nb)O_2$, but not here. This does not arise from a different screening due to the variation of ionization degree because there is no change of valence degree and there is no effect at the Ti edge. It remains that this effect is due to an M-M interaction which occurs between vanadium atoms and not

between titanium atoms. V-V distances are probably close to the Ti-Ti length for low vanadium content and split into 0.265 and 0.312 nm is VO_2. This change is related to antiferromagnetic coupling between V $3d^1$ ions.

On the other hand, comparison of the energy position of the various XANES features on both edges (Ti and V) shows that

$$E_V(X)-E_{Ti}(X)=498.3+0.2 \text{ eV}$$

for X is a peak label ($X=B,C1,C2',C2''$).

The local potential splits into two terms: one that is identical on all metallic sites and another which can be called the disorder potential. The first gives the overall shape of the edge and is related to long-range order. The second is a perturbation that gives the vanadium or titanium character to the edge shape. It is expected that the perturbation is smaller in the high-energy part of the spectrum. 498.3 eV would then be the difference between the two $1s$ metal orbitals and between the screening at the Ti or V center. If high-energy transition at the Ti and V edges arise from the same levels, this means that the t_{2g} levels of V are $1.0+0.1$ eV below the t_{2g} level of titanium regardless of the vanadium content. This observation agrees well with the evolution of the flat-band potential in $(Ti,V)O_2$, which decreases by almost 1 eV from TiO_2 to $(Ti_{0.4}V_{0.6})O_2$.[26] This agrees also with optical spectroscopy,[27] which shows the appearance of a d band 1 eV below the direct band-to-band transition in TiO_2.

V. CONCLUSIONS

By an improved smoothing procedure we have obtained, by second-derivative analysis, reliable measurements of energy positions and of the full width at half maximum of the various transitions occurring on the titanium or vanadium absorption spectra.

Only small changes in either energy positions or intensities are detectable for high-energy transitions (i.e., above $1s\rightarrow 4s$). We have concluded that no electron transfer occurs between titanium and vanadium. A different result was obtained on Ti spectra in $(Ti,Nb)O_2$.[24] Coincidence of XANES features corresponding to delocalized wave functions on the Ti and V edges implies that the t_{2g} levels of vanadium are 1 eV below the t_{2g} levels of titanium. This observation explains why electrons are localized, why no valence change occurs, and why the conductivity is activated.

On the other hand, small shifts in the $1s\rightarrow 4p$ peak versus $1s\rightarrow t_{2g}$, depending on the vanadium content, seem to follow the relation suggested by Natoli using the mean radius of the metal-oxygen bond, but other transitions do not. Nevertheless, it seems that the titanium octahedron is less squeezed than the vanadium octahedron. This distortion cannot be the cause of the decrease in the crystal-field splitting, since squeezing gives rise to an increase. It is more likely that V-V interactions lead to a 1 eV decrease in the $1s\rightarrow t_{2g}$ and $1s\rightarrow e_g$ splitting at the V edge and not at the Ti edge.

For all compositions, an excitonic peak is present even in VO_2, for which it was not mentioned previously. The intensity and the binding energy of this narrow feature are well correlated with an increase of the $3d$ electrons on the vanadium.

Finally, for vanadium content smaller than 80%, solid solutions are rutile, whereas they are monoclinic above this concentration, but this phase transition is not detectable on the edge structure because it corresponds to a small distortion which leads to splittings well below the resolution of x-ray-absorption spectroscopy. On the other hand, the structural evolution around titanium and around vanadium seems to be different. Titanium is rather unperturbed by the V-V interactions when the vanadium chain length increases progressively to infinity as in VO_2.

ACKNOWLEDGMENTS

We would like to thank Jacqueline Petiau, Robert Cortes, and Jose Goulon for their discussions and technical assistance. The Laboratoire des Composés Non-Stoechiométriques is "Unité No. 446 associée au Centre National de la Recherche Scientifique."

[1]T. Horlin, T. Niklewski, and M. Nygren, J. Phys. (Paris) Colloq. **37**, C4-C9 (1976).
[2]M. G. Blanchin, E. Vicario, and R. A. Ploc, J. Appl. Crystallogr. **10**,228 (1977).
[3]Ed Caruthers and L. Kleinman, Phys. Rev. B **7**, 3760 (1973).
[4]C. Sommers, R. de Groot, D. Kaplan, and A. Zylberstein, Phys. (Paris) Lett. **36**, L157 (1975).
[5]D. Paquet and P. Leroux-Hugon, J. Magn. Magn. Mater. **15**, 999 (1980).
[6]J. F. Marucco, B. Poumellec, and F. Lagnel (unpublished).
[7]J. F. Marucco, B. Poumellec, and F. Lagnel, J. Mater. Sci. Lett. **5**, 99 (1986).
[8]J. Wong, F. W. Lytle, R. P. Messmer, and D. H. Maylotte, Phys. Rev. B **30**, 5596 (1984).
[9]B. Poumellec, J. F. Marucco, and B. Touzelin, Phys. Status Solidi B **437**, 366 (1986).
[10]L. A. Grunes, Phys. Rev. B **27**, 2111 (1983).
[11]A. Bianconi, Phys. Rev. B **26**, 2741 (1982).
[12]K. Vos, J. Phys. C **10**, 3917 (1977).
[13]N. Daude, C. Gout, and C. Jouanin, Phys. Rev. B **15**, 3229 (1977).
[14]A. D. Burton and P. A. Cox, Philos. Mag. B **51**, 255 (1985).
[15]F. W. Kutzler and D. E. Ellis, Phys. Rev. B **29**, 6890 (1984).
[16]R. A. Bair and W. A. Goddard III, Phys. Rev. B **22**, 2767 (1980).
[17]J. Pascual, J. Camassel, and H. Mathieu, Phys. Rev. Lett. **39**, 1490 (1977).
[18]I. K. Kristensen, J. Appl. Phys. **39**, 5341 (1968).
[19]W. Rudorff, G. Walter, and J. Stadler, Z. Anorg. Allg. Chem. **297**, 1 (1958).
[20]B. Poumellec and R. Tetot, unpublished results (available from authors).
[21]D. W. Fisher, Phys. Rev. B **5**, 4219 (1972).
[22]N. Kosugi, T. Yokoyama, and H. Kuroda, in *EXAFS and*

Near Edge Structure III, edited by K. O. Hodgson, B. Hedman, and J. E. Penner Hahn (Springer-Verlag, Berlin, 1984), p. 55.

[23]C. R. Natoli, in *EXAFS and NES III,* edited by K. O. Hodgson, B. Hedman, and J. E. Penner Hahn (Springer-Verlag, Berlin, 1984), p. 38.

[24]B. Poumellec, F. Lagnel, J. F. Marucco, and B. Touzelin, Phys. Status Solidi B **133**, 371 (1986).

[25]N. I. Lazukova and V. A. Gubanov, Solid State Commun. **20**, 649 (1976).

[26]J. Gautron, P. Lemasson, B. Poumellec, and J. F. Marucco, Solar Energy Mater. **9**, 101 (1983).

[27]K. Sakata, Phys. Status Solidi B **116**, 145 (1983).